

LDV Measurements in the Endwall Region of an Annular Turbine Cascade Through an Aerodynamic Window

G. V. Hobson* ,
W. H. Donovan** and J. D. Spitz***

Department of Aeronautics and Astronautics
Naval Postgraduate School
Monterey, CA 93943

Abstract

Laser-Doppler velocimetry measurements through a one millimeter hole in the casing of an annular turbine cascade were performed in the endwall region downstream of the blade row. Complementary three-hole pressure probe measurements were also taken downstream of the nozzle blades, as well as blade surface pressure measurements. The object of this study was to devise methods for the measurement close to an endwall and to overcome the problems associated with optical access window contamination. The eventual aim of the project was to perform laser anemometry measurements in the tip leakage region of an operating turbine of comparable size. Good comparisons with numerical predictions of the flowfield were also obtained.

Nomenclature

P	static pressure
Pt	stagnation pressure
Po	reference stagnation pressure
Prat	inlet total -to-exit static (at the hub) pressure ratio
U	mean axial velocity
u'	fluctuating axial velocity
V	mean circumferential velocity
Vexit	maximum exit plane velocity
v'	fluctuating circumferential velocity
X	axial direction
Y	tangential direction

Introduction

This paper reports the endwall region laser-Doppler-velocimeter measurements of the flow downstream of an annular turbine stator. The object of this study was to devise a method of measurement close to the endwall, and to overcome the problems of contamination of the optical access window. The size and scale (232.9 mm diameter annulus and 17.7 mm blade height) of the rig was purposely limited so that experience could be gained in performing measurements in such a confined

space prior to taking measurements in a newly commissioned turbine test rig (TTR). The test article to be used in the TTR is the first stage Alternate Turbine Design (ATD), of the High Pressure Fuel Turbopump (HPFTP) for the Space Shuttle Main Engine (SSME). The size and scale of the current turbine cascade and the ATD are similar. Ultimately the aim was to obtain measurements close to or in the tip leakage region of the rotor blades.

The annular turbine cascade was designed for laser-Doppler-velocimetry and was constructed so that measurements could be made in the endwall region of the exit passage one half an axial chord downstream of the blades. Two-component measurements of the Mach number, flow angle and turbulence intensity were obtained through a 1.09 mm opening in the endwall at depths ranging from 0.01 mm to 3.34 mm. Tangential surveys were performed over two blade passages by rotating the turbine nozzle circumferentially. The measurements were compared to fully three-dimensional numerical predictions [Refs. 1 & 2]. Additional predictions were also made, over a wide operating range of the turbine nozzle, of the midspan blade surface pressure measurements.

Good comparisons, between the measured and predicted blade surface pressure distributions, were obtained over all the operating pressures. The lowest pressure ratio (exit static at the hub - to - inlet total pressure) of 0.507 yielded a choked nozzle with locally supersonic flow over the aft portion of the blades. Again good comparisons were made between the predicted and measured blade surface pressures at these conditions.

LDV measurements were performed at the highest pressure ratio of 0.9054, or lowest exit Mach number equal to 0.38 with a fiber optics probe system. The probe volume (0.1 mm x 1.5 mm) passed cleanly through the optical access hole and radial surveys were conducted to depths dictated by the half angle of the beams, which were 3.8 degrees.

Previous LDV measurements in an annular turbine cascade have been carried out at NASA Lewis Research

* Associate Professor, Member AIAA

** Lt. US Navy

*** LCDR. US Navy

Center in a large scale rig with various nozzle geometries [Refs. 3 - 5]. The measurements were performed with a single component LDV at different orientations to resolve the various velocity components.

Experimental Apparatus

The Annular Turbine Cascade (ATC) was developed to provide a small-scale device for flow field measurements. Thomas [Ref. 6] developed the basic apparatus, which is shown schematically in Fig. 1. The inner hub radius was 98.8 mm with constant blade geometry to the outer

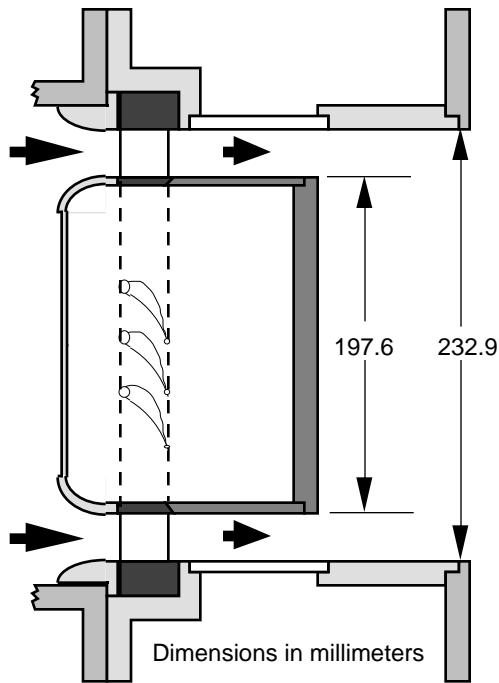


Fig 1. Annular turbine cascade cutaway

radius of 116.5 mm. The stator row had 31 blades with a midspan spacing of 21.8 mm resulting in a solidity of 1.73. The blade profile and coordinates are presented in Fig. 2. Blade surface pressure measurements were performed with static pressure ports on either side of a single blade passage [Ref. 7]. Seven suction-side and four pressure-side ports, each 0.4 mm in diameter, were drilled at midspan.

Total pressure, Mach number and flow angle measurements were performed with a three-hole cobra probe, one half of an axial chord downstream of the trailing edge of the blade row [Ref. 8]. The exit static pressure on the hub was also measured at this axial station, and the inlet total pressure and temperature were recorded approximately ten axial chords ahead of the leading edge of the blades.

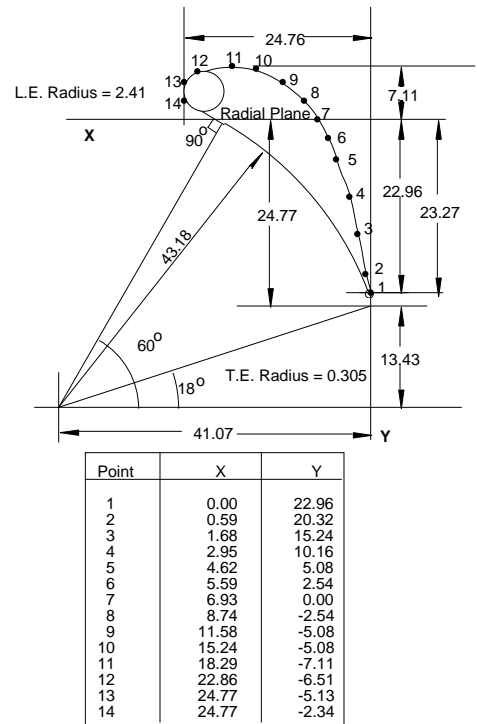


Fig 2. Blade geometry

A removable alignment blank with a 1.09 mm (0.043") hole drilled through it such that the hole was located one half of an axial chord downstream of the blade trailing edges was used as the optical access window [Ref. 8]. This provided the ability to perform endwall flow measurements to depths of 3 mm as shown in figure 3 below.

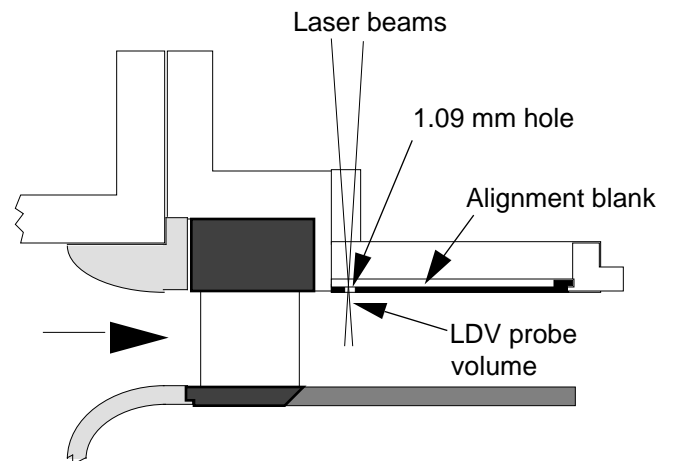


Fig 3. Optical access through an aerodynamic window. Circumferential surveys were performed by rotating the cross-hatched section of the cascade i.e. the blade row and center section. This was performed in one degree

increments and a total of 17 degrees was surveyed. One blade passage was 11.6 degrees in extent.

The LDV system is shown schematically in Figure 4. A Lexel 4 Watt laser was connected to a multicolor beam separator which divided the incoming light into shifted (40 Mhz) and unshifted beams. the two beams were further split into three polarized pairs: green (514 nm wavelength), blue (488 nm) and violet (476 nm). Only two component measurements were performed with the green and blue beams. Couplers directed each beam to

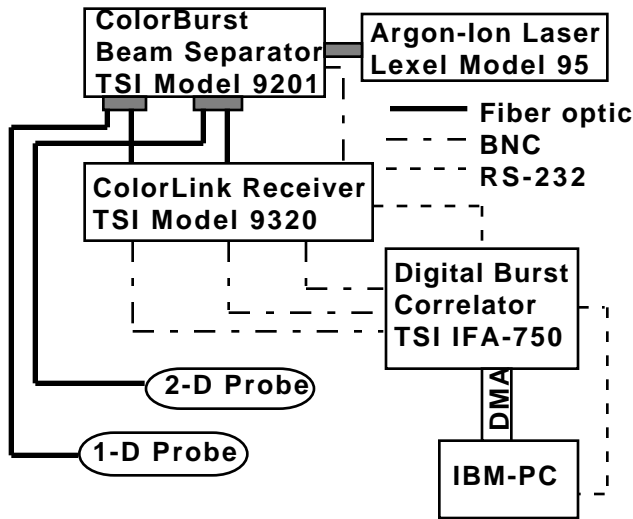


Fig 4. LDV system schematic

the laser probe via a fiber-optic cable. Each probe contained receiving optics (backscatter mode) which directed the reflected light off 1 μm oil mist particles to the photomultipliers in the receiver. Analog Doppler bursts were then sent to the burst spectrum analyzer for digitizing. Digitized data was transferred via a direct memory access cable to a Personal Computer, which also performed control functions on the various instruments.

Results and Discussion

Blade surface pressure distributions

The numerical prediction of the flowfield through the annular turbine cascade was initiated [Ref. 8] before the blade midspan surfaces were instrumented for pressure measurements [Ref. 7]. Thus the computations, which are compared to experiment in Fig. 5, were truly a prediction. As can be seen both the suction side (lower trace) and pressure side (upper trace) were well predicted and that the suction-surface curve showed that the passage throat was at 0.8 of axial chord. After the

throat the flow decelerated slightly to 0.9 of axial chord where it once again reaccelerated to a minimum suction pressure close to the trailing edge of the blade. This reacceleration was most probably due to the continued curvature of the suction surface at the trailing edge. The three-hole (cobra) probe measurements were performed at this pressure ratio, and numerical results (computed at the same time as the data was taken) were also compared to those data.

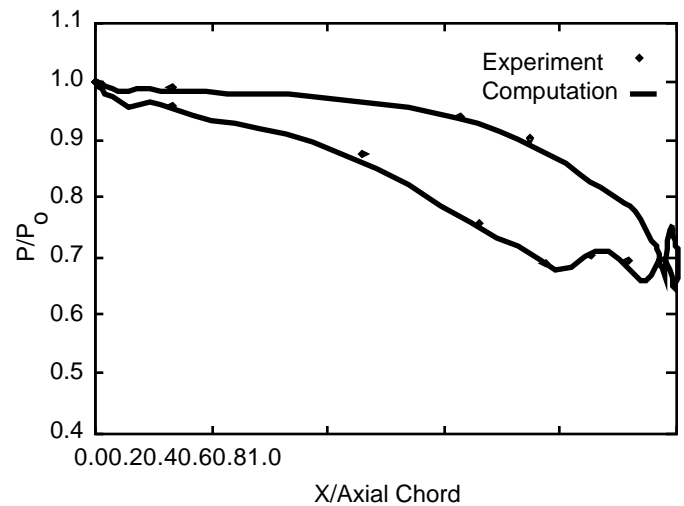


Fig 5. Prediction of blade surface pressure distribution ($Prat = 0.6815$).

A full range of pressure ratios was tested up to choking of the nozzle, and these are compared in pairs in Figs. 6

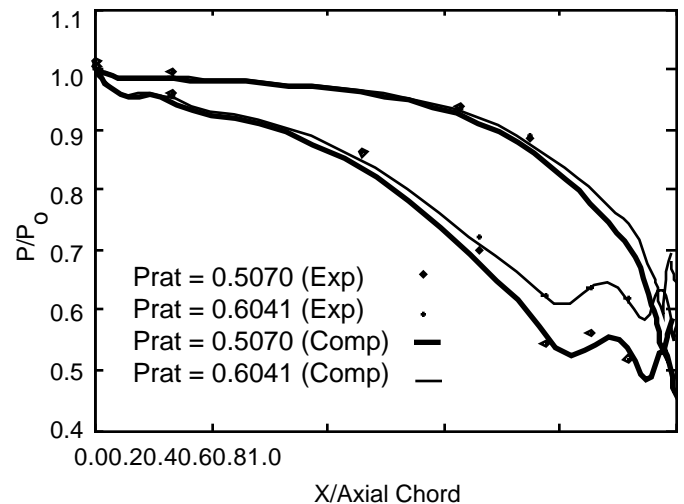


Fig. 6. Blade surface pressure distributions (high Mach nos.)

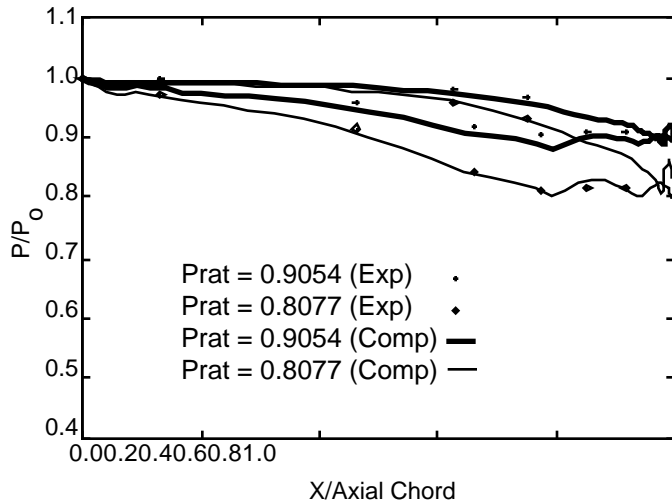


Fig. 7. Blade surface pressure distributions (low Mach nos.)

and 7. Figure 6 shows the two higher exit Mach number flows, one at choke and the other just before the throat went sonic. The numerical solution for the choked case showed subsequent trailing edge shocks which extended across the wake of the adjacent blade, out of the exit plane of the computational grid. The shock interaction with the wake caused the wake to narrow down, resulting in a wake which was repeatedly diffusing then contracting. As with the high Mach no. cases the low exit Mach no. test cases showed the same overall trend in blade loading. Good overall agreement resulted between the numerical results and the experimental data. The lowest pressure ratio (0.9054) tested was the pressure ratio used for all the LDV measurements.

Exit plane probe surveys

Three-hole probe surveys were obtained at an average Reynolds number of 650 000 based on axial chord. The pressure ratio was set at 0.6815 to enable proper comparisons with the CFD solution. This gave an exit Mach number of approximately 0.7. Eighteen circumferential positions of the blade row were sampled at four radial locations. The Mach no. comparisons of the four spanwise locations were made in fig. 8. Wake-profile phase coincidence was established using the 50% span Mach number data. The phase was kept constant for the circumferential comparisons at all other spanwise locations. Initially at 25% span the comparison was off by almost 20%, however close to the casing (90% span) the numerical results are within 5% of the experimental data. This improved comparison gave confidence in the ability of the code to predict the casing endwall flow. This feature was useful in assisting in the interpretation of the endwall LDV measurements.

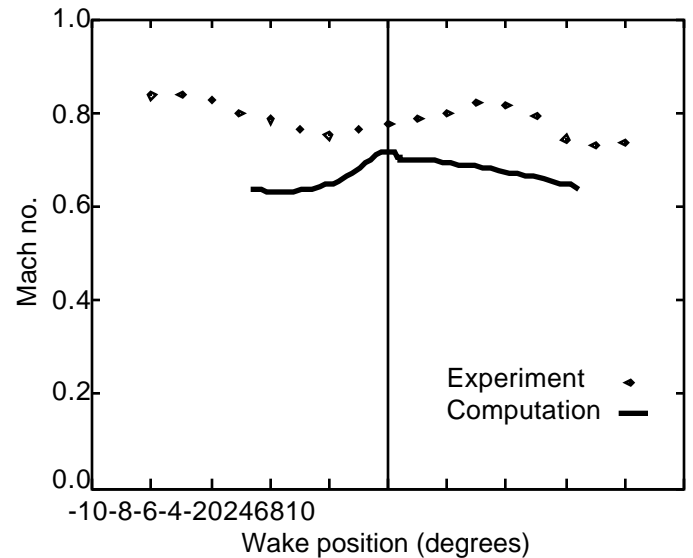


Fig 8a. Mach no. comparison, 25% span

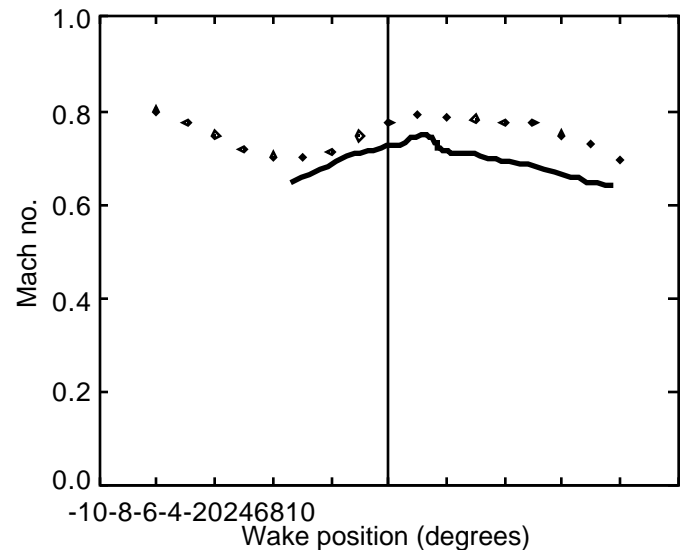


Fig 8b. Mach no. comparison, 50% span

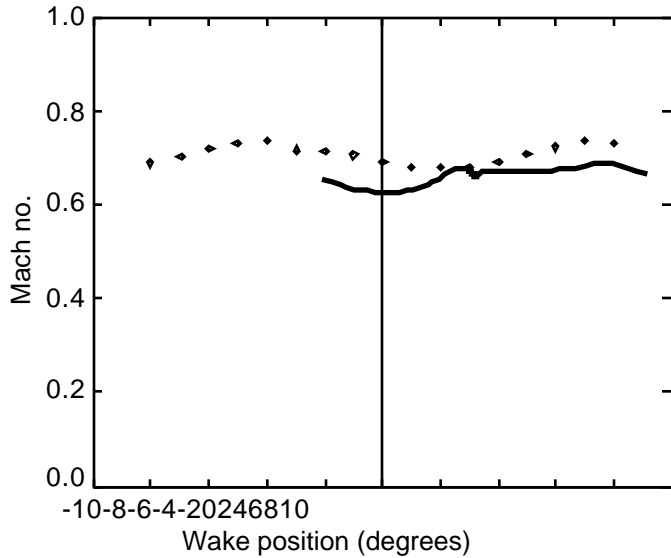


Fig 8c. Mach no. comparison, 75% span

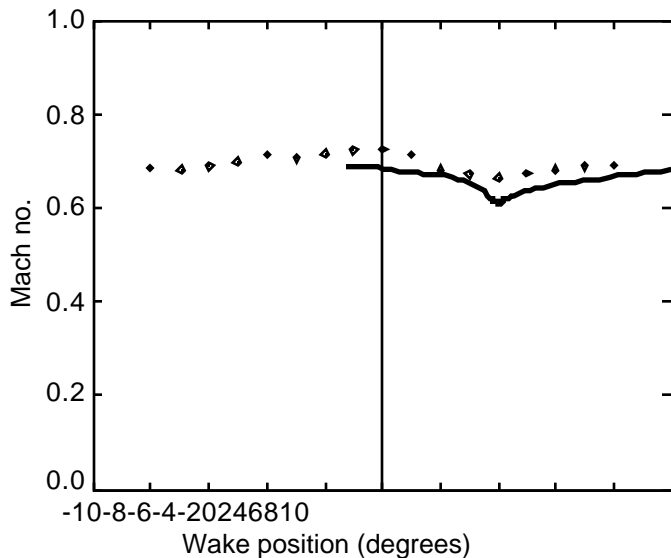


Fig 8d. Mach no. comparison, 90% span

Endwall LDV measurements

Laser-Doppler-velocimetry measurements were performed at the highest pressure ratio of 0.9054. Measurements were taken over a circumferential range of 17 degrees in one-degree increments. The Mach number distribution is shown in the figure 9 which does not show any significant endwall boundary layer profile or blade wake profiles. This could be due to velocity biasing of the data in the probe volume as a result of the significant spatial error. The wakes had also mixed out by this station leaving a relatively uniform velocity distribution. In the center of the survey grid (at 0 degrees wake position) there was evidence of the core flow with

wakes on either side. Flow periodicity was also evident in the contour plots.

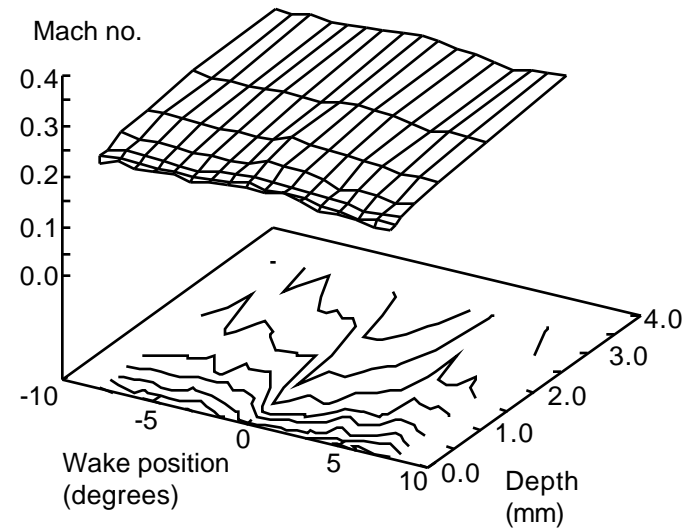


Fig 9. Endwall Mach no. distribution

Periodicity was also evident in the plot for the flow angle (fig. 10) which was defined as the arc tangent of the circumferential velocity and the axial velocity as measured by the two-component LDV probe. Flow angle varied between 75 and 77 degrees for the area surveyed.

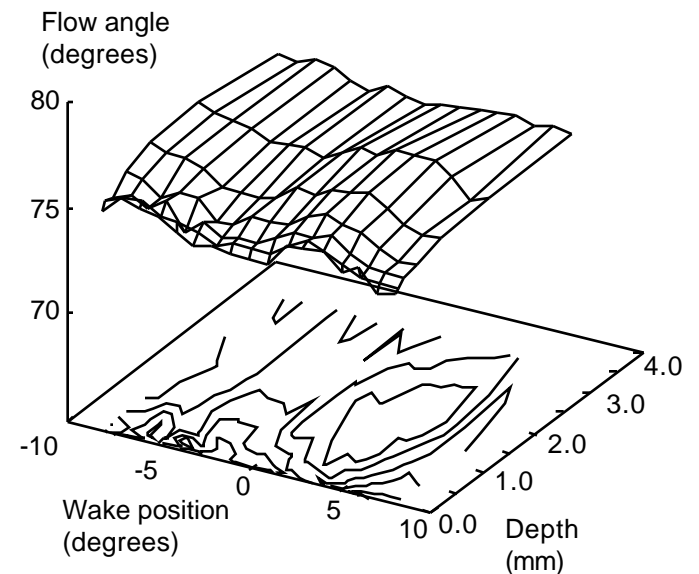


Fig 10. Endwall flow angle distribution
The associated turbulent kinetic energy field is shown in figure 11, where the percent turbulent kinetic energy is defined as;

$$\frac{1}{2} \frac{(u^2 + v^2)}{V_{exit}^2}$$

where V_{exit} is the maximum total velocity at the exit survey plane. The inlet freestream turbulence intensity was measured to be approximately 2% with the ATC removed from the rig. The turbulence field showed periodicity more significantly than the mean flow data, as the turbulence peaked in the two wakes over which the survey was conducted. The turbulence peaked to an overall maximum of approximately 0.5 in the endwall boundary layer. This peak was located at the second spanwise station of 99% span, the closest (to the endwall) survey being conducted at 99.9% span.

Percent turbulent kinetic energy

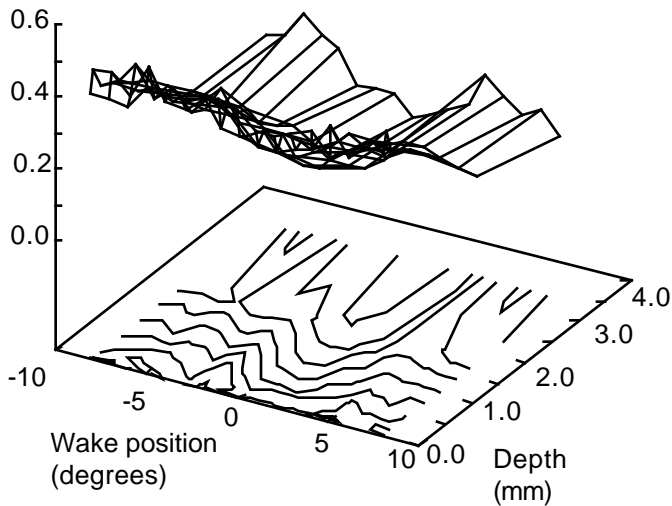


Fig 11. Endwall turbulent kinetic energy distribution

The experimental and computational measurements were phase locked (using the maximum total Mach no.) circumferentially at the 80.9% span location. After viewing other circumferential surveys at different spanwise locations it was determined that this was the best location to perform phase locking of the data. The results of this comparison are shown in figure 12a. The phase of the locking was kept constant for all other spanwise locations. The 80.9% spanwise location corresponded to the maximum LDV probe immersion of 3.34 mm. Figure 12b shows the Mach number comparison at the 0.89 mm immersion .

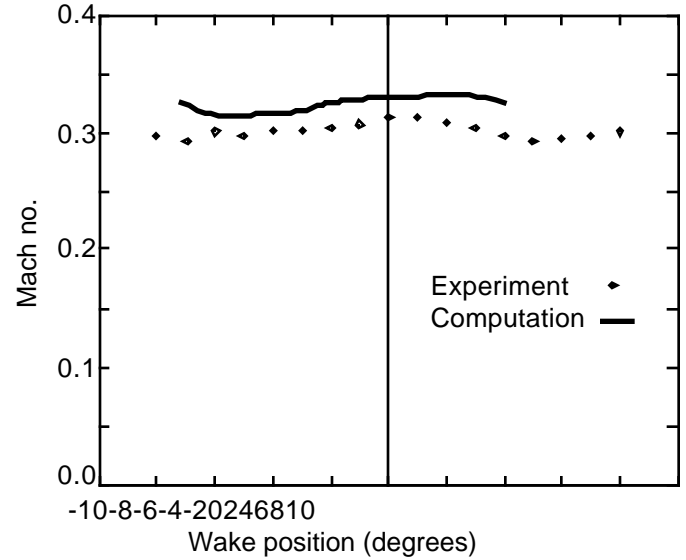


Fig 12a. Mach no. comparison, 80.9% span.

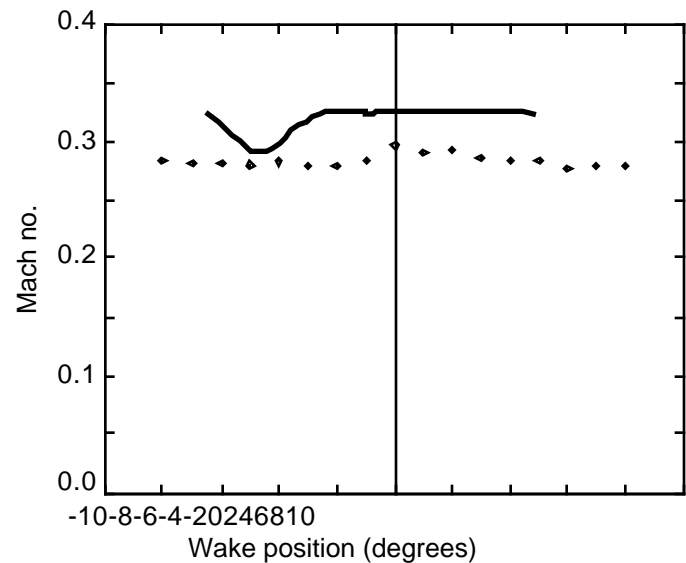


Fig 12b. Mach no. comparison, 94.9% span.

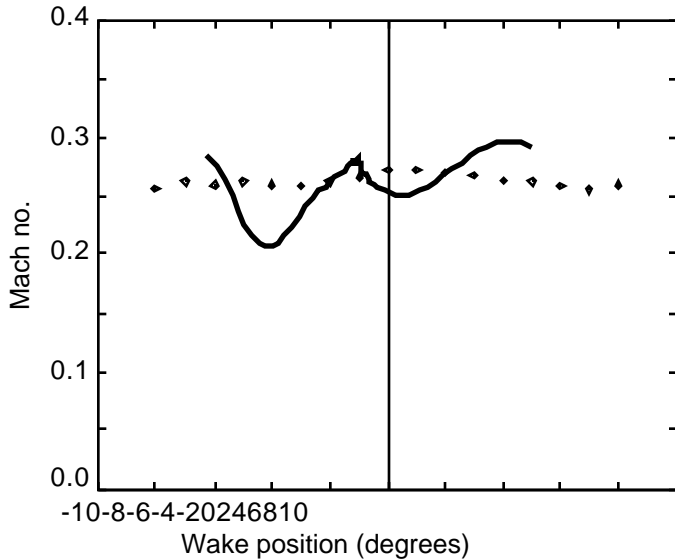


Fig 12c. Mach no. comparison, 99.0% span.

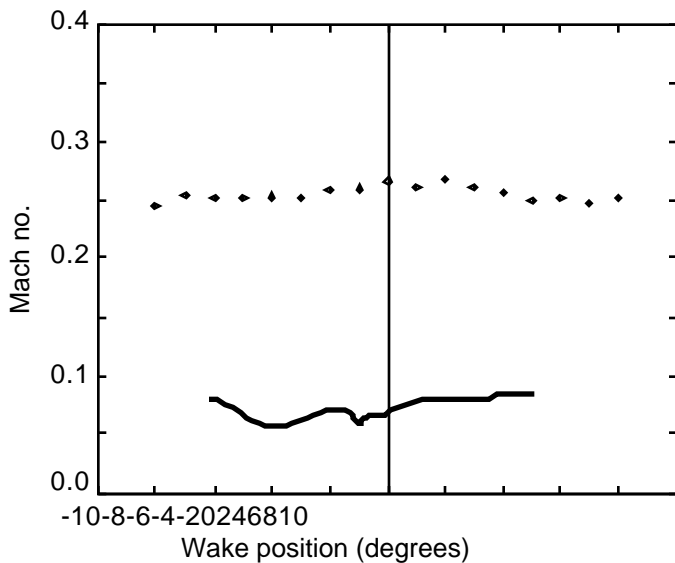


Fig 12d. Mach no. comparison, 99.9% span.

Figure 12c shows the Mach number comparison at the 0.18 mm immersion. Computed Mach numbers differed from experimental values by an average 13% between the surveys at 0.18 mm and 3.34 mm. The difference increased to 71% near the endwall (fig. 12d), possibly due to a combination of LDV data velocity biasing and insufficient grid resolution of the numerical results. Velocity biasing was estimated to cause an approximate 11% velocity increase in the endwall region. The numerical solution at the endwall (0.01 mm) was from the next to last grid surface from the endwall.

The question of radial spatial error with the probe volume needed to be determined. The probe volume length and diameter (figure 13) was calculated as 1.56 and 0.11 mm respectively. The probe volume had 32 fringes across

the minor axis, however after data processing by the burst spectrum analyzer an average of 13 fringe crossings constituted a valid Doppler burst. This was because the processor sampled the center of the overall burst. An effective probe volume size was then obtained which slightly reduced the spatial error.

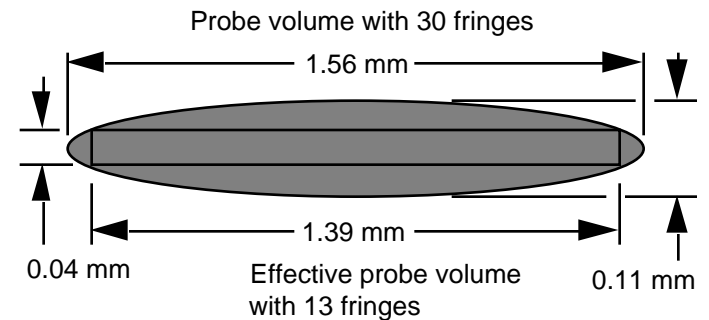


Fig 13. Probe volume dimensions

Figure 14 depicts, to scale, the radial survey locations and resolution that resulted from the endwall depths and effective probe volume dimensions. The lack of spatial resolution most probably contributed the most to the lack of agreement between the Mach number profiles at the endwall.

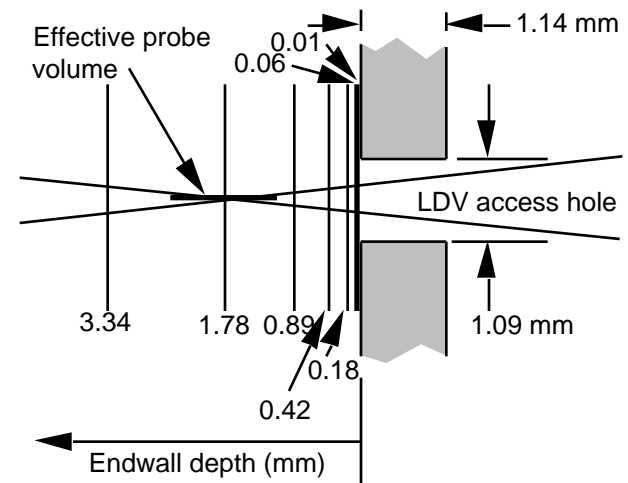


Fig 14. Endwall measurements schematic

The hole, or aerodynamic window, was vented to atmosphere so that flow did exit from the opening. The estimated pressure ratio across the hole was 100 mm of water (or 0.01 atmospheres). This would certainly have affected the measurements, however it is felt that this was only the case very close to the endwall (i.e. the effect of the sink flow exiting the annulus was localized), and that the effect on the seeding particles would have been even less.

Acknowledgement

The present study was supported by the Naval Air Warfare Center Aircraft Division, Patuxent River, with Deborah Parish as contract monitor.

Conclusions

Experimental measurements of blade midspan surface pressures were obtained and favorably compared with numerical predictions over a wide range of subsonic and transonic conditions. Full three-dimensional flowfield calculations were compared to probe measurements at the exit plane of the annular cascade, at the design pressure ratio. These comparisons improved considerably toward the endwall region, thus giving confidence in using numerical predictions to assist in the interpretation of the LDV measurements close to the endwall. The LDV measurements were performed at a higher pressure ratio which resulted in lower exit Mach numbers, however the complexity of flowfield was similar to the high Mach number test case.

No significant wakes appeared in the mean flow LDV data, however the turbulence profiles showed wake periodicity. The turbulent kinetic energy data also showed a ridge of maximum values in the endwall boundary layer, which dropped off slightly at the endwall. The comparison of computational and experimental results yielded an average 13% difference in Mach number. All experimental measurements were repeatable to an average uncertainty of approximately 7% for velocity, flow angle and turbulence intensity.

Finally it was felt that this method of endwall measurements could be viable in actual turbines, which operate at elevated temperatures making it difficult if not impossible to insert optical windows through which LDV measurements can be made.

References

1. Chima, R. V. and Yokota, J. W., "Numerical Analysis of Three-Dimensional Viscous Flows in Turbomachinery," *AIAA Journal*, Vol. 28, No. 5, pp 798-806, May 1990.
2. Chima, R. V., "Viscous Three-Dimensional Calculations of Transonic Fan Performance," presented and published for the AGARD 7th Propulsion and Energetics Panel Symposium on CFD Techniques for Propulsion Applications, San Antonio
3. Goldman, L. J. and Seasholtz, R. G., "Laser Anemometer Measurements in an Annular Cascade of Core Turbine Vanes and Comparison with Theory," NASA TP 2018, June 1982.
4. Goldman, L. J. and Seasholtz, R. G., "Three Component Laser Anemometer Measurements in an Annular Cascade of Core Turbine Vanes with Contoured End Wall," NASA TP 2846, November 1988.
5. Goldman, L. J. and Seasholtz, R. G., "Laser Anemometer Measurements and Computations in an Annular Cascade of High Turning Core Turbine Vanes," NASA TP 3252, July 1992.
6. Thomas, G. D., "Measurements and Prediction of the Flow Through an Annular Turbine Cascade," Master of Science in Aeronautical Engineering, Naval Postgraduate School, Monterey, California, March 1993.
7. Donovan, W. H., "Experimental and Computational Investigation of Flow Through an Annular Turbine Cascade," Master of Science in Aeronautical Engineering, Naval Postgraduate School, Monterey, June 1995.
8. Spitz, J. D., "Laser Anemometry and Viscous Computation of the Flow Through an Annular Turbine Cascade," Master of Science in Aeronautical Engineering, Naval Postgraduate School, Monterey, March. 1994.